

Atomic-orbital analysis of the Cu Fermi surface by two-dimensional photoelectron spectroscopyFumihiko Matsui,^{1,2,*} Hiroaki Miyata,³ Oliver Rader,⁴ Yohji Hamada,⁵ Youjiro Nakamura,⁶ Koji Nakanishi,⁵ Koji Ogawa,⁵ Hidetoshi Namba,⁵ and Hiroshi Daimon^{1,2,5}¹Graduate School of Materials Science, Nara Institute of Science and Technology (NAIST), Ikoma, Nara 630-0192, Japan²CREST-JST, Japan³Toray Research Center, Ohtsu, Shiga 520-8567, Japan⁴BESSY, Albert-Einstein-Str. 15, D-12489, Berlin, Germany⁵Ritsumeikan University, Kusatsu, Shiga 525-8577, Japan⁶JEOL, Akishima, Tokyo 196-8558, Japan

(Received 19 October 2004; revised manuscript received 23 May 2005; published 18 November 2005)

A method for atomic-orbital orientation determination at each k point has been developed. The three-dimensional Cu Fermi surface (FS) structure was measured and visualized by stacking a series of photoelectron intensity angular distribution (PIAD) at different photon energies. PIADs from the Cu(001) surface were obtained using a display-type analyzer and linearly polarized synchrotron radiation. The atomic orbitals composing the FS were determined to be mainly $4p$ orbitals with their axes pointing outward. Atomic orbital orientations at different k coordinates on FS as well as the FS cross-section structures were revealed directly from experiment and were confirmed by *ab initio* calculation.

DOI: [10.1103/PhysRevB.72.195417](https://doi.org/10.1103/PhysRevB.72.195417)

PACS number(s): 73.20.At, 71.18.+y, 79.60.-i, 71.15.Ap

I. INTRODUCTION

The analysis of the Fermi surface (FS) is essential for the study of all kinds of physical properties of metals, e.g., electronic and magnetic properties, chemical reactivities, and the optical response. The increasing demand to investigate the unique physical and chemical properties of new materials like the high- T_C superconductors has led to a rapid evolution of Fermiology by high-resolution photoemission studies with synchrotron radiation¹⁻³ (SR). The method is based on the fact that angle-resolved photoelectron spectroscopy gives direct access to the FS defined in k space and its use has been demonstrated in a number of cases.⁴⁻⁹

Recently, research has been touching upon several problems where in addition to the shape of the FS, knowledge about the atomic orbitals constituting the FS and their orientation would be desirable. To name one example, the FS of a liquid lead monolayer supported on a Cu(111) surface has been measured most recently.¹⁰ It was reported that different sheets of the FS have distinct coherence lengths and this finding has been attributed to a strong dependence of the localization lengths on the character of the constituent atomic orbitals.¹⁰ Another example is the FS of a 1.2 monolayer Ni film on Cu(100) which has been found to be similar to the bulk Ni FS (Ref. 11), although the electronic structure of the Ni monolayer is different from that of bulk Ni.¹² In similar transition-metal films, coupling of the electronic structure to the Cu(100) substrate was discussed in conjunction with atomic-orbital composition based on band structure calculations.⁴ Yet another example is the unusual behavior of surface states on stepped Cu(111) surfaces.^{13,14} Here, a strong tilt of orbital orientation was recently predicted at the step edges.¹⁵ Furthermore, the key role of the atomic orbital degree of freedom in the science and technology of correlated electrons, regarded as “orbitronics,” has been one of the stimulating issues in the latest frontiers of solid state

physics.¹⁶ These examples illustrate the demand for a direct experimental method to analyze the atomic orbitals resolved in three-dimensional k space. Nevertheless, such method was still lacking and is the topic of the present report.

FS mapping has typically been performed with a small acceptance angle energy analyzer by rotating a sample holder on a goniometer. For example, several groups have mapped the FS of Cu using a narrow energy window by rotating the sample.^{4,5} When combined with a tunable SR, various cross sections of the three-dimensional FS can be obtained.^{17,18}

In the rotating-sample method, the azimuthal symmetry information of initial state (magnetic quantum number m) in the photoelectron intensity angular distribution (PIAD) is lost during the sample rotation. An alternative to the above method is a two-dimensional photoelectron spectroscopy (2D-PES) using a display-type analyzer which can acquire a full image of the PIADs in a narrow energy window at one time.^{7-9,19} Recently, we have proposed a new method, the orbital determination from angular distribution (ODAD), to analyze the component ratio among atomic orbitals, such as p_z or $d_{x^2-y^2}$, from PIADs obtained by using linearly polarized SR and a display-type analyzer.²⁰ This analysis is based on the idea that the PIAD can be represented as a product of the one-dimensional density of states (1D-DOS) and angular distribution from atomic orbitals (ADAO). This analysis has successfully described experimental data from many different systems, such as graphite,^{21,22} $\text{Bi}_2\text{Sr}_2\text{CaCu}_2\text{O}_8$,²³ and TaSe_2 .²⁴

In the general case, the materials are not layered like the above mentioned examples and a dispersion along the k_z direction perpendicular to the surface has to be taken into account. The three-dimensional Cu FS has been surveyed by a series of PIAD measurements at various photon energies. Here, we present the analysis of atomic orbitals constituting the Cu FS by 2D-PES combined with linearly polarized SR.

II. EXPERIMENTAL DETAILS

The experiment was performed at the linearly polarized soft x-ray beamline BL-7 of Ritsumeikan SR Center in Shiga, Japan.²² The range of photon energies ($h\nu$) covered by a modified Rowland mount spherical-grating monochromator is 35–130 eV. The chamber base pressure was $\sim 7 \times 10^{-11}$ Torr. The Cu(001) single crystal sample was cleaned *in situ* by repeated cycles of Ar^+ bombardment and annealing to 600 °C. The surface quality was checked by low energy electron diffraction and ultraviolet photoelectron spectroscopy.

The ODAD analysis from PIAD is most effectively done by using linearly polarized light and a display-type analyzer. SR is introduced through a hole in the outer sphere of the analyzer and is perpendicularly incident on the sample surface. The direction of the electric vector of the SR is horizontal. The PIAD at a particular kinetic energy is projected onto a fluorescent screen with the emission angle preserved. Thus, the momentum of the photoelectrons parallel to the surface can be deduced directly from the position of the PIAD peak on the screen. The energy and the angular resolution of this analyzer are 1% and 1° , respectively. The raw images were normalized by the analyzer transmittance angular distribution. The averaged pattern of the secondary electrons was used as the analyzer transmittance pattern. Typical acquisition time for one PIAD was 5 min.

In order to confirm the result of atomic-orbital analysis from measured PIADs, the atomic-orbital component ratio distribution in k space is calculated using *ab initio* code WIEN2K.²⁵ This uses the full-potential augmented plane wave plus (APW+LO) method²⁶ with the generalized gradient approximation (GGA).²⁷ The muffin-tin radii R_{MT} for Cu atoms were 2.0 a.u. The cutoff of the plane-wave expansion K_{max} was 3.5.

III. MEASUREMENT OF FERMI SURFACE

A series of PIADs shown in Fig. 1 was measured using photons of energy from 40 to 80 eV. The periphery corresponds to the emission angle of $\sim \pm 40^\circ$ from the surface normal. These PIADs contain information on the shape and the symmetry of atomic orbitals composing the Cu sp band at the Fermi level. The $[110]$ direction of the Cu surface coincides with the electric vector of the incident light indicated as a horizontal arrow in the figure.

All the PIADs show twofold symmetry due to the linear polarization of the incident light. For instance, four bright segments appear along the sides of a diamond in the PIAD of photon energy 41.5 eV. As the photon energy increases, the segments move inward. The PIAD at 55.5 eV photon energy shows a nearly circular feature with breaks at upper and lower directions. Further, it gradually turns into a square-like shape at 61.5 eV. Photoelectron intensities seen outside of the square at the photon energy of 71.5 eV correspond to the “necks” between neighboring Brillouin zones (BZs). Finally the pattern in the first BZ converges to two spots and then disappears.

Qu *et al.* also have reported PIADs with light incident at an angle of 45° to the surface normal.¹⁷ The trend seen in the

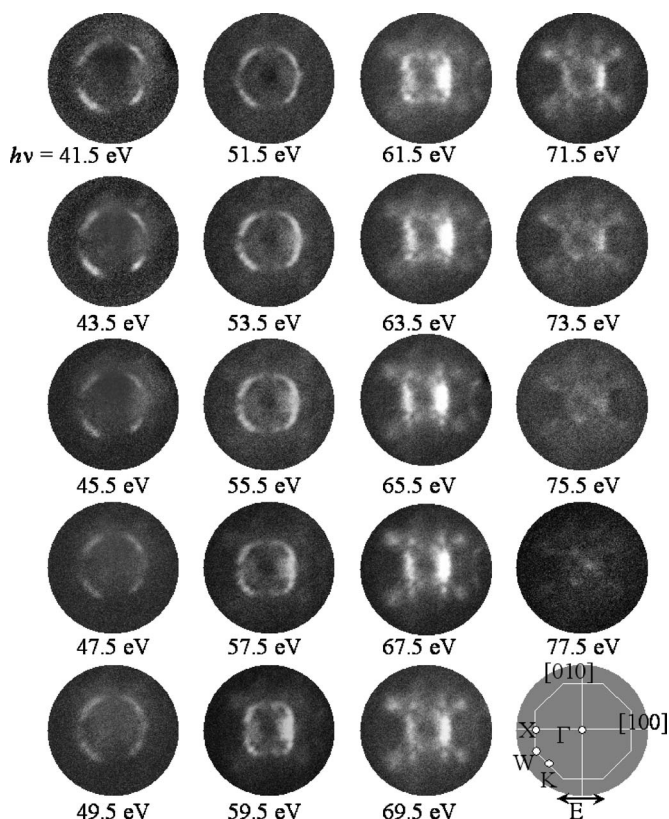


FIG. 1. PIADs from the Fermi level of Cu(001) surface excited by a normal-incident linearly polarized light. The electric vector of the incident light is in the horizontal direction.

above series of PIADs is consistent with their observation using photon energy of 95 eV for the excitation where the photoelectron intensity from the first BZ is considerably suppressed. In particular, the dependence of the PIAD on the photon polarization is clearly observed in the present case and, as will be shown below, contains information on atomic orbital of initial state.

We have also calculated the Cu FS using *ab initio* code.²⁵ Figure 2(a) shows the Cu FSs and BZs arranged in a bcc lattice. The narrow part connecting neighboring Cu FSs along the Γ - L direction is often called a neck. On the other hand, there are protrusions in the Γ - X directions.²⁸ The characteristic shape appearing in the cross section at the (110) plane is known as a “dog bone” structure.^{4–6}

The radii of the four spherical curved surfaces drawn around the BZ labeled B represent the wave vectors of the photoelectrons excited from the Fermi level with photons of 41.5, 51.5, 61.5, and 71.5 eV. The origin of the vector is set at the center of the BZ labeled A . A work function of 4.7 eV and an inner potential of 8.5 eV are assumed for calculating each wave number.¹⁷ Intersection of sphere and FS indicates the emission angle of photoelectron. Note that the sphere representing the excitation by photons of 71.5 eV touches the FS in the BZ labeled D .

Figures 2(b)–2(e) are the combination of the above calculation and actual PIADs. The FS labeled B and C in Fig. 2(a) are shown in Figs. 2(b) and 2(c), while the FS labeled B and D are shown in Figs. 2(d) and 2(e).

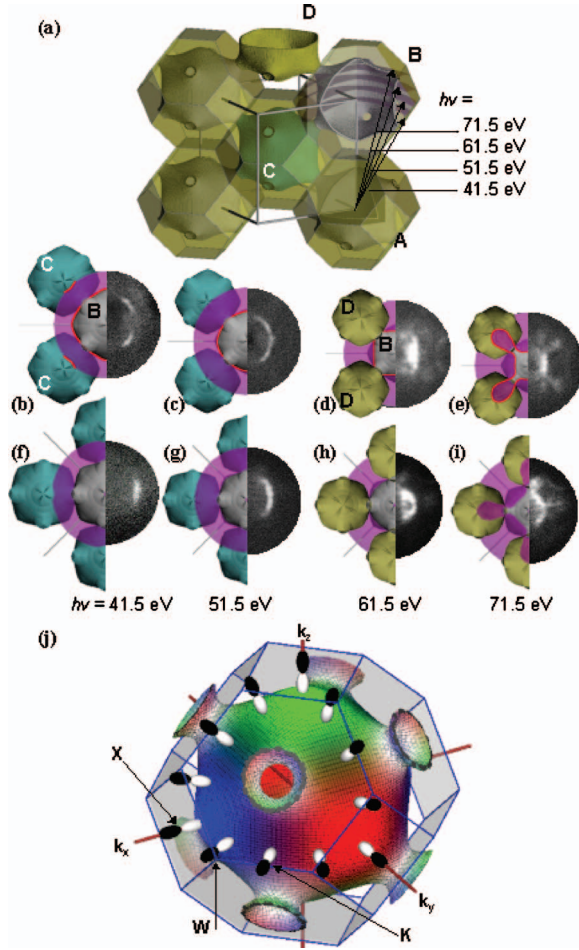


FIG. 2. (Color) (a) The Cu FS together with the spheres corresponding to the wave vector of photoelectrons excited with various photon energies. (b)–(e) The top views of Cu FSs and the spheres representing the photoelectron wave vectors together with observed PIADs. FSs labeled *B* and *C* are shown in (b) and (c), while FSs labeled *B* and *D* are shown in (d) and (e). (f)–(i) Same as (b)–(e), but for sample rotated by 45°. (j) The Cu FS with atomic orbitals constituting each point in k space. The direction of the p orbital axes pointing outward is derived from the experimental analysis. FS is colored according to the $4p$ orbital ratio distribution calculated by using the *ab initio* code. Blue, red, and green colors correspond to $4p_x$, $4p_y$, and $4p_z$ orbitals, respectively.

The sphere for photoelectrons excited by photons of 41.5 eV crosses FS near the ΓXWK plane. The cross section in the BZ labeled *B* shows a diamond-like shape. The maxima in the PIAD corresponds to the cross section at the Γ -*K* direction. In the case of excitation by photons of 51.5 eV, the cross section becomes more circular shaped, showing good agreement with observed PIAD. The sphere for photoelectrons excited by photons of 61.5 eV crosses the FS near *L* points. The cross section of the FS at the BZ labeled *B* shrinks and becomes square-like. Finally, the neighboring BZs are observed in the PIAD excited by photons of 71.5 eV. The wave number reproducing PIAD in Fig. 2(e) is about 3% larger than the wave number of photoelectron assuming inner potential of 8.5 eV. This is mainly due to the limited energy resolution of the measurement. This

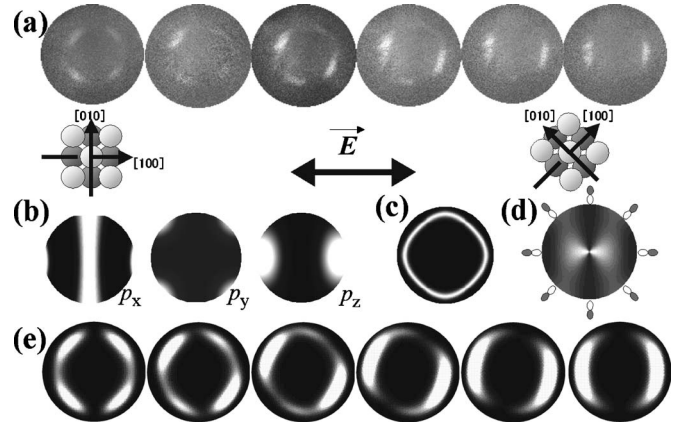


FIG. 3. (a) PIADs with various azimuthal rotation angles. Photon energy of 45 eV is used for exciting the electrons of FS in the ΓXWK plane. (b) ADAO from p_x , p_y , and p_z orbitals. (c) Cross section of the FS at the ΓXWK plane. (d) and (e) ADAO and simulated PIADs from p orbitals with their axes pointing radially, respectively.

neck structure has also been reported by Aebi *et al.*⁵ They used He *I* (21.2 eV) for excitation. This corresponds to the lower part of the FS in the same BZ.

IV. PRINCIPLE OF ORBITAL DETERMINATION

The analysis of the PIAD from a tight-binding approximated valence band and a Bloch-wave final state showed that the photoelectron intensity $I(\theta, \phi)$ in the direction of polar angle θ ($\theta=0^\circ$ at surface normal $[001]$ direction) and azimuthal angle ϕ ($\phi=0^\circ$ at horizontal $[100]$ direction) can be expressed as

$$I(\theta, \phi) \propto D^1(k_{\parallel}) \left| \sum_{\nu} A_{\nu} \right|^2, \quad (1)$$

where $D^1(k_{\parallel})$ is the 1D-DOS (Ref. 29) and $|A_{\nu}|^2$ is the ADAO from the ν th atomic orbital ψ_{ν} .³⁰ $A_{\nu}(\theta, \phi)$ for s and p orbitals in the case of normal incidence can be expressed as

$$A_s = \langle \psi_{E_k, \mathbf{k}} | \boldsymbol{\epsilon} \cdot \mathbf{r} | \psi_{2s} \rangle \propto \sin \theta \cos \phi,$$

$$A_{p_x} = \langle \psi_{E_k, \mathbf{k}} | \boldsymbol{\epsilon} \cdot \mathbf{r} | \psi_{2p_x} \rangle \propto 2(1 - 3 \sin^2 \theta \cos^2 \phi),$$

$$A_{p_y} = \langle \psi_{E_k, \mathbf{k}} | \boldsymbol{\epsilon} \cdot \mathbf{r} | \psi_{2p_y} \rangle \propto 3 \sin^2 \theta \sin 2\phi,$$

$$A_{p_z} = \langle \psi_{E_k, \mathbf{k}} | \boldsymbol{\epsilon} \cdot \mathbf{r} | \psi_{2p_z} \rangle \propto 6 \cos \theta \sin \theta \cos \phi. \quad (2)$$

$|A_{\nu}|^2$ for p orbitals are depicted in Fig. 3(b). For instance, the ADAO from the p_z orbital has a zero intensity line along the vertical direction ($\phi = \pm 90^\circ$) and maxima in two directions of $\phi = 0$ and 180° . These features are observed in the PIADs excited by photons of 61.5 eV or higher in Fig. 1. These PIADs correspond to the cross section of the FS around the *X* point.

On the other hand, A_{p_y} has its maxima in four directions of $\phi = 45^\circ, 135^\circ, 225^\circ,$ and 315° . The PIADs excited by 40

~ 50 eV photons corresponding to the cross section of the FS near ΓXWK plane have such characteristic features. However, we cannot simply conclude that the constituting atomic orbital at the FS within the ΓXWK plane is p_y , since the Cu(001) surface has fourfold symmetry.

To determine the constituting atomic orbitals at each k point, we have measured the PIADs with rotating azimuthal angles ϕ_s . Photons of 45 eV are used to excite the FS just in the ΓXWK plane. Figure 3(a) shows the PIADs with rotating ϕ_s from 0° to 45° in 9° steps from left to right in counter-clockwise direction. The p_y -like pattern (maxima in four directions) observed at the angle of $\phi_s=0^\circ$ becomes a p_z -like pattern (maxima in two directions) at the angle of $\phi_s=45^\circ$. The photoelectron intensity for the $[\bar{1}\bar{1}0]$ and $[\bar{1}\bar{1}0]$ directions is weak at $\phi_s=0^\circ$ and becomes strong at $\phi_s=45^\circ$, while the photoelectron intensity for the $[110]$ and $[\bar{1}\bar{1}0]$ directions diminishes at $\phi_s=45^\circ$. The photoelectron intensity for the $[100]$, $[\bar{1}00]$, $[010]$, and $[0\bar{1}0]$ directions remains weak at all angles.

Several conformations of atomic orbitals including contribution of s orbital had been tested but only one of them showed good agreement with the observed PIADs. Figure 3(c) is the calculated cross section of the FS. Figure 3(d) shows the derived arrangements of p orbitals together with the contour map of ADAO calculated using the following equation:

$$|A_{\text{Fermi}}(\theta, \phi)|^2 = |A_{p_x}(\theta, \phi)\cos \phi + A_{p_y}(\theta, \phi)\sin \phi|^2. \quad (3)$$

Figure 3(e) is the series of simulated PIADs corresponding to the observed ones in Fig. 3(a). D^1 and $|A_{\text{Fermi}}|^2$ are essential in this characteristic rotational dependence, i.e., the different ϕ_s dependence for the $[100]$ and $[110]$ directions is due to the variance in the emission angle θ .

Variations of PIADs with a sample rotated by 45° are shown in Figs. 2(f)–2(i). The p_z -like features observed in the PIAD ($\phi_s=0^\circ$) excited at photon energy of 51.5 eV or higher remain also at the angle of $\phi_s=45^\circ$. The FS of Cu is concluded to be composed of $4p$ orbitals with their axes pointing outward from the Γ point.

In Fig. 2(j), the directions of p orbitals at various points on the FS revealed from experimental atomic-orbital analysis are depicted. For example, p_x , p_y , and p_z orbitals are placed in the $[100]$, $[010]$, and $[001]$ directions, respectively. On the other hand, FS is colored according to the $4p$ orbital ratio distribution calculated by using the forementioned *ab initio* code. Blue, red, and green colors correspond to $4p_x$, $4p_y$, and $4p_z$ orbitals, respectively. The calculated $4p$ orbital ratio distribution shows good agreement with the result of the atomic-orbital analysis from present measured PIADs.

Moreover, the contributions of $4s$ and $3d$ orbitals to Fermi surface were calculated. For example, the partial densities of state for $4s$, $4p$, and $3d$ orbitals at the Fermi surface near the X point were 0.18%, 0.53%, and 0.29%, respectively. We attribute the reason why the s -orbital contribution did not appear in the PIAD analysis to the small photoemission cross section of s orbitals at a photon energy of 45 eV. Contributions of each d orbital could not be determined due to ambiguity.

V. CONCLUSIONS

A method for analyzing the atomic orbitals of crystals at each k point has been developed. The three-dimensional structure of Cu FS was explored by use of a display-type analyzer and linearly polarized SR. Comparing observed PIADs and simulated ones using transition matrix elements and FS cross section calculated, the atomic orbitals constituting the FS were found to be aligned with their axes pointing outward. Furthermore, the atomic-orbital component ratio distribution in k space is calculated using *ab initio* code based on the full-potential APW+LO method. Good agreement between the results of experimental and theoretical atomic-orbital mapping in k space confirms the validity of the present method, which provides key information for the orbitronics science and technology.

The authors express sincere thanks to the staff of the SR Center, Ritsumeikan University. O. R. was supported by the A. v. Humboldt Foundation.

*Electronic address: matui@ms.naist.jp

¹S. Hüfner, *Photoelectron Spectroscopy* (Springer-Verlag, Berlin, 1995).

²J. C. Campuzano, A. Kaminski, H. Fretwell, J. Mesot, T. Sato, T. Takahashi, M. Norman, M. Randeria, K. Kadowaki, and D. Hinks, *J. Phys. Chem. Solids* **62**, 35 (2001).

³T. Greber, T. J. Kreuzer, and J. Osterwalder, *Phys. Rev. Lett.* **79**, 4465 (1997).

⁴M. Hochstrasser, N. Gilman, R. F. Willis, F. O. Schumann, J. G. Tobin, and E. Rotenberg, *Phys. Rev. B* **60**, 17030 (1999).

⁵P. Aebi, J. Osterwalder, R. Fasel, D. Naumović, and L. Schlapbach, *Surf. Sci.* **307–309**, 917 (1994).

⁶J. A. Con Foo, A. P. J. Stampfl, A. Ziegler, B. Mattern, M. Holering, R. Denecke, L. Ley, J. D. Riley, and R. C. G. Leckey,

Phys. Rev. B **53**, 9649 (1996).

⁷H. Daimon, *Rev. Sci. Instrum.* **59**, 545 (1988).

⁸T. Düttemeyer, C. Quitmann, M. Kits, K. Dörnemann, L. S. O. Johansson, and B. Reihl, *Rev. Sci. Instrum.* **72**, 2633 (2001).

⁹M. Kotsugi, W. Kuch, F. Offi, L. I. Chelaru, and K. Kirschner, *Rev. Sci. Instrum.* **74**, 2754 (2003).

¹⁰F. Baumberger, W. Auwärter, T. Greber, and J. Osterwalder, *Science* **306**, 2221 (2004).

¹¹G. J. Mankey, K. Subramanian, R. L. Stockbauer, and R. L. Kurtz, *Phys. Rev. Lett.* **78**, 1146 (1997).

¹²C. Pampuch, O. Rader, R. Kläsches, and C. Carbone, *Phys. Rev. B* **63**, 153409 (2001).

¹³A. P. Shapiro, T. Miller, and T-C. Chiang, *Phys. Rev. B* **38**, 1779 (1988).

- ¹⁴J. E. Ortega, S. Speller, A. R. Bachmann, A. Mascaraque, E. G. Michel, A. Narmann, A. Mugarza, A. Rubio, and F. J. Himpsel, *Phys. Rev. Lett.* **84**, 6110 (2000).
- ¹⁵R. Eder and H. Winter, *Phys. Rev. B* **70**, 085413 (2004).
- ¹⁶Y. Tokura and N. Nagaosa, *Science* **288**, 462 (2000).
- ¹⁷Z. Qu, A. Goonewardene, K. Subramanian, J. Karunamuni, N. Mainkar, L. Ye, R. L. Stockbauer, and R. L. Kurtz, *Surf. Sci.* **324**, 133 (1995).
- ¹⁸E. W. Plummer and W. Eberhardt, *Adv. Chem. Phys.* **49**, 533 (1982).
- ¹⁹T. Nohno, F. Matsui, Y. Hamada, H. Matsumoto, S. Takeda, K. Hattori, and H. Daimon, *Jpn. J. Appl. Phys., Part 1* **42**, 4756 (2003).
- ²⁰H. Daimon, M. Kotsugi, K. Nakatsuji, T. Okuda, and K. Hattori, *Surf. Sci.* **438**, 214 (1999).
- ²¹H. Nishimoto, T. Nakatani, T. Matsushita, S. Imada, H. Daimon, and S. Suga, *J. Phys.: Condens. Matter* **8**, 2715 (1996).
- ²²F. Matsui, Y. Hori, H. Miyata, N. Suga, H. Daimon, H. Totsuka, K. Ogawa, T. Furukubo, and H. Namba, *Appl. Phys. Lett.* **81**, 2556 (2002).
- ²³M. Kotsugi, H. Daimon, K. Nakatsuji, T. Okuda, T. Furuhashi, M. Fujikawa, H. Takagi, Y. Tezuka, S. Shin, K. Kitahama, T. Kawai, and S. Suga, *J. Electron Spectrosc. Relat. Phenom.* **88–91**, 489 (1998).
- ²⁴T. Okuda, K. Nakatsuji, S. Suga, Y. Tezuka, S. Shin, and H. Daimon, *J. Electron Spectrosc. Relat. Phenom.* **101–103**, 355 (1999).
- ²⁵P. Blaha, K. Schwarz, G. K. H. Madsen, D. Kvasnicka, and J. Luitz, *WIEN2k, An Augmented Plane Wave Plus Local Orbitals Program for Calculating Crystal Properties* (Vienna University of Technology, Austria, 2001).
- ²⁶E. Sjöstedt, L. Nördstrom, and D. Singh, *Solid State Commun.* **114**, 15 (2000).
- ²⁷J. P. Perdew and Y. Wang, *Phys. Rev. B* **45**, 13244 (1992).
- ²⁸N. W. Ashcroft and N. D. Mermin, *Solid State Physics* (Holt, Rinehart and Winston, New York, 1976).
- ²⁹T. Grandke, L. Ley, and M. Cardona, *Phys. Rev. B* **18**, 3847 (1978).
- ³⁰S. M. Goldberg, C. S. Fadley, and S. Kono, *J. Electron Spectrosc. Relat. Phenom.* **21**, 285 (1981).